then, that the geometry change between excited and ground states would occur as a motion along only $\nu_4$ in the ground state, and along both $\nu_4$ and $\nu_7$ in the excited state. Such a change in the normal modes would explain why $\nu_7$ is strong only in absorption.

The $^1n \rightarrow \pi^*$ electronic transition is formally allowed, yet quite weak ($f \simeq 2 \times 10^{-4}$). We observe that all of the totally symmetric FC progressions appear to be more intense in absorption. This could imply that these excited-state vibrations are active in borrowing oscillator strength from some higher electronic state of the same A″ symmetry.

There is no evidence in our data concerning the fate of the eclipsed excited state conformer. In the gas phase the eclipsed conformer actually lies several hundred $cm^{-1}$ *below* the staggered conformer. This is a puzzling result. Gordon et al., studying condensed pure $CF_3NO$ at 77 K, observed system II but not system I absorption. They suggested that the eclipsed isomer is somehow strongly blue shifted and broadened (perhaps entirely eliminated?) in condensed phase. This suggestion is difficult to understand theoretically. Recall that the eclipsed or staggered FCNO unit is rotating as a whole with respect to the neon host. Therefore, why should solvation have essentially no effect on both the eclipsed ground state and the staggered excited state, and yet strongly modify the eclipsed excited state?

Normally, drastic spectral changes accompany a drastic change in the *electronic* wave function, rather than a change in the size or conformation as determined by the geometry of the nuclei. For example, excited Rydberg[14] and charge-transfer[15] states have been observed to appreciably shift and broaden in rare gas hosts. One might conjecture that system I bands actually terminate on an electronically different excited singlet state. However, this possibility seems remote in view of extensive ab initio SCF CI calculations on $CH_3NO$ that show only one excited singlet state below 7.14 eV.[16]

One might propose that in the gas phase the eclipsed conformer is nonfluorescent and in addition does not radiationlessly "feed" the fluorescent staggered conformer. In this case our data would not contradict the idea of negligible solvent effect, since we have no evidence that any change has occurred in going from gas phase to solid neon. However, negligible solvent effect is not consistent with the conclusion of Gordon et al., that system I bands are strongly blue shifted in condensed $CF_3NO$. It is also difficult to understand why an unperturbed eclipsed conformer would be nonfluorescent, as the rate of radiationless transition into the eclipsed ground state should be similar to that of the observed fluorescent staggered conformer. Similar rates are expected if the geometry changes in the CNO chromophore upon electronic excitation are essentially the same.

We conclude that either the eclipsed conformer is strongly solvated for some unexplained reason, or the system I bands are hot bands of system II despite the conclusion of Gordon et al. Upon completion of this work, we learned of preliminary results by Spears and co-workers which suggest that system I bands actually are hot bands. If this is true then our expectation that either conformer would be negligibly solvated is correct.

### References and Notes


(1) R. G. Gordon, S. C. Dass, J. R. Robins, H. F. Shurvell, and R. F. Whittock, *Can. J. Chem.*, **54**, 2660 (1976). The ground-state torsional barrier $V_0$ has been measured to be 269 ± 17 $cm^{-1}$ by P. H. Turner and A. P. Cox, *Chem. Phys. Lett.*, **39**, 585 (1976). The ground-state torsion rotational constant is $F = 2.44$ $cm^{-1}$, as determined by the observed geometry. These values yield a torsional frequency of $\omega = 77$ $cm^{-1}$ via $\omega = 3\sqrt{V_0 F}$.
(2) J. Goodman and L. E. Brus, *J. Chem. Phys.*, **65**, 1156 (1976).
(3) J. Mason, *J. Chem. Soc.*, 3904 (1957).
(4) K. G. Spears and L. Hoffland, *J. Chem. Phys.*, **66**, 1755 (1977).
(5) P. J. Carmichael, B. G. Gowenlock, and C. A. F. Johnson, *J. Chem. Soc., Perkin Trans. 2*, 1853 (1973).
(6) L. E. Brus and V. E. Bondybey, *J. Chem. Phys.*, **65**, 71 (1976).
(7) B. DiBartolo and R. C. Powell, "Phonons and Resonances in Solids", Wiley, New York, N.Y., 1976, Chapters 10 and 11. The ZPL transition produces the solvent directly in its new equilibrium configuration around the excited guest. The lattice phonon wing maximum is the vertical, Franck–Condon transition which leaves the solvent configuration unchanged during guest excitation. Potential energy curves for molecules in solids are properly constructed from ZPL positions only (see ref 6).
(8) This statement only applies to valence (not Rydberg) excited states.
(9) In solid $H_2$ host, detailed spectra in the $12_0^0$ region were not obtained.
(10) A. C. Albrecht, *J. Mol. Spectrosc.*, **6**, 84 (1961).
(11) V. E. Bondybey and L. E. Brus, *J. Chem. Phys.*, **64**, 3724 (1976).
(12) B. Dellinger and M. Kasha, *Chem. Phys. Lett.*, **38**, 9 (1976).
(13) H. F. Shurvell, S. G. Dass, and R. G. Gordon, *Can. J. Chem.*, **52**, 3149 (1974).
(14) J. Goodman and L. E. Brus, to be published.
(15) J. Goodman and L. E. Brus, *J. Chem. Phys.*, **65**, 3808 (1976).
(16) T. K. Ha and U. P. Wild, *Chem. Phys.*, **4**, 300 (1976).


# A Method of Describing the Charge Distribution in Simple Molecules


**Peter A. Kollman**

*Contribution from the Department of Pharmaceutical Chemistry, School of Pharmacy, University of California, San Francisco, California 94143.*

*Received May 16, 1977*


**Abstract:** We present a simple method of representing the charge distribution in small molecules and apply the derived charge distributions to analyze the electrostatic potentials near these molecules as well as the structures and energies of intermolecular complexes. The molecules and ions discussed here are HF, $H_2O$, $NH_3$, HCl, $H_2S$, $H_3P$, $F_2$, $H_2$, $N_2$, $Cl_2$ $SO_2$, $CO_2$, HCN, HNC, $H_2CO$ (ground and excited states), $H_2NCHO$, $CH_4$, $CHF_3$, $NH_4^+$, $Li^+$, $F^-$, $CH_3NH_2$, $CH_3OH$, $CH_3F$, $C_2H_4$, and $C_2H_2$.


## Introduction

One of the goals of a chemist is to determine charge distributions in molecules. A knowledge of the charge distribution allows one to learn a great deal about its tendency to undergo covalent and noncovalent interactions with other molecules. In this paper, we focus on noncovalent interactions and ask ourselves the question: what is the simplest method of representing the charge distribution which can qualitatively reproduce the magnitude and directionality of the electrostatic potential as well as the magnitude and directionality of inter-

0002-7863/78/1500-2974$01.00/0 

**Table I.** Parameters for First and Second Row Hydrides

| $AH_n$[a] | $X$(A)[a] | $\mu$(exp)[b] | $d$(AH), Å[c] | $\theta$(HAH), deg[d] | $d$(bp), Å[e] | $\mu$(bp)[f] | $\mu$(lp)[g] | $\theta$(lp), deg[h] | $d$(lp), Å[i] | $r$(vdW), Å[j] |
|---|---|---|---|---|---|---|---|---|---|---|
| HF | 4.1 | 1.82 | 0.917 | | 0.597 | 1.33 | 0.49 | 60.0 | 0.031 | 1.35 |
| $H_2O$ | 3.5 | 1.85 | 0.957 | 104.5 | 0.588 | 1.28 | 0.57 | 57.3 | 0.055 | 1.4 |
| $H_3N$ | 3.07 | 1.47 | 1.01 | 106.7 | 0.588 | 0.90 | 0.57 | | 0.059 | 1.5 |
| HCl | 2.83 | 1.08 | 1.275 | | 0.717 | 0.76 | 0.32 | 70.0 | 0.031 | 1.8 |
| $H_2S$ | 2.44 | 0.97 | 1.328 | 92.2 | 0.698 | 0.45 | 0.52 | 64.5 | 0.062 | 1.85 |
| $H_3P$ | 2.06 | 0.58 | 1.421 | 93.3 | 0.687 | −0.37 | 0.95 | | 0.098 | 1.9 |

[a] $X$ = electronegativity; $X$(H) = 2.2, see ref 15. [b] Experimental dipole moment in debyes. [c] Experimental A–H bond distance. [d] Experimental HAH angle. [e] Distance of bond pair from the hydrogen. [f] Bond pair dipole moment. [g] Lone pair dipole moment. [h] Location of lone pair relative to dipolar axis of molecule. [i] Distance of lone pair from A in electron pair representation. [j] Distance of partial charge from A in van der Waals representation; see ref 15 for van der Waals radii used.

molecular complexes found in accurate quantum mechanical calculations.

We have shown,[1,2] following the suggestion by Bonaccorsi et al.,[3] that the electrostatic potential[4] and its gradient[4] are an extremely useful guide to thinking about many different types of noncovalent interactions, including H bonds, "Li bonds", ion–neutral interactions, "charge transfer" complexes, and van der Waals complexes. In addition it was found,[2] using the Morokuma component analysis,[5] that the electrostatic energy was usually a very good guide in determining the minimum energy structural parameters, with the exception of the molecule–molecule separation. To predict the separation, all energy components, including electrostatic, exchange repulsion, polarization, and charge transfer, are important.[6]

Nonetheless, we feel that it is worthwhile focusing on the electrostatic properties of molecules because one can use them with surprising accuracy (a) to predict directionality of intermolecular complex formation and (b) to predict relative interaction energies in intermolecular complexes.

There are a number of simple approaches to "analyzing" intermolecular complex formation. They range from a strictly empirical approach by Drago and co-workers,[7] which uses experimental enthalpies of complex formation to derive empirical parameters characteristic of each acid and base, to more semiquantitative conceptual approaches such as the Mulliken two-determinant "charge transfer" model,[8] which relates the strength of electron donor–acceptor complexes to the ionization potential of the electron donor and the electron affinity of the electron acceptor; and Allen's H-bond model,[9] which focuses on the ionization potential of the electron donor and the bond dipole of the proton donor as the key features of the hydrogen bond.

We feel that an electrostatic approach has the capability of correctly representing the relative structures and energies of many weak and moderate strength intermolecular complexes to qualitative accuracy. In the early studies of H bonds, much was made of the role of charge redistribution and the failure of electrostatic models to predict, for example, that amines were better Lewis bases than nitriles, despite their smaller dipole moments.[10] It is clear from recent studies[2] that this objection to electrostatic approaches is not valid because the a point dipole moment is only the very crudest representation of the charge distribution. Below we seek simple charge distributions which are consistent with both the molecular dipole moment and more accurate quantum mechanical calculations.

### Methodology and Studies of HF, $H_2O$, $NH_3$, HCl, $H_2S$, and $PH_3$

Our basis for the choice of an "electron pair" representation of the charge distribution comes from a qualitative expectation that such a representation is required to "explain" the experimental[11] and theoretical[12] result that in

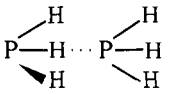

$\theta \sim 60°$. In fact, the electrostatic energy appears to have a minimum energy very close to that of the total energy,[2,13] suggesting that the charge distribution of isolated HF can be used to rationalize the minimum energy $\theta$. An atom-centered partial charge representation $H^{\delta+}$–$F^{\delta-}$ would predict a linear ($\theta = 0$) dimer.

Our first question is: Where do we place the electron pairs? (a) The $\sigma$ electron pair: we reason that in an A–B bond, the $\sigma$ electron pair should be located nearer the more electronegative atom; in fact, a simple empirical estimate for its location is

$$d = d_{AB}\frac{X(A)}{X(A) + X(B)} \quad (1)$$

where $d$ is the distance of the $\sigma$ bond pair from the less electronegative atom B, $d_{AB}$ is the AB bond length, $X$(A) is the electronegativity of A, and $X$(B) is the electronegativity of B. For HF, $d_{AB}$ = 0.917 Å, $X$(A) = 4.1, $X$(B) = 2.2; this leads to a $d$ = 0.602 Å and a bond moment of 1.44 D. A similar placement of the bond electron pairs in the other hydrides leads to the results shown in Table I. It is pleasing that this simple empirical choice of placement of bond moments is qualitatively consistent with the analysis of Cotton and Wilkinson,[14] i.e., both bond moments and lone pair moments contribute significantly to the overall dipole moment. (b) The placement of the lone pairs (lp)? For $H_3N$ and $PH_3$, we place them at a distance $d$(lp) to reproduce the molecular dipole moment. However, for $H_2O$, $H_2S$, HF, and HCl, we must determine an appropriate angle and distance for our lone pairs relative to the dipolar axis. For $H_2O$ and $H_2S$, we use the angle appropriate for $sp^3$ hybridization with the bond pairs along the bond directions. This leads to values for $\theta$ of 57.3° for $H_2O$ and 64.5° for $H_2S$. We then place the lone pairs at a distance from the atom ($d$) to reproduce the overall experimental dipole moment. For HF we use $\theta$ = 60°, which is consistent with the minimum energy angle found in experiments and theoretical calculations on $(HF)_2$. For HCl, we use the fact that $\theta$ would be expected to be greater than that of HF by approximately the difference found in $H_2S$ and $H_2O$ and use $\theta$ = 70°. The distances $d$(lp) which are consistent with the experimental dipole moments are listed in Table I. Because the above full lone pair representation was not very successful in reproducing the quantum mechanical electrostatic potentials (see below), we also explored four other types of charge distribution (Figure 1b–e). First, we considered a representation (b) where the bond dipole is represented by partial charges rather than centered on the atoms by an electron pair located along the bond axis. This reduces the charges needed to represent the bond charge distribution and for analysis of intermolecular interactions seems to be more useful. Two other possible alternatives in the

Table II. Electrostatic Potentials[a] at Reference Positions for the Hydrides $NH_3$, $H_2O$, $HF_3$, $PH_3$ $H_2S$, and HCl

| Molecule | Charge distribution[c] (a) | (b) | (c) | (d) | (e) |
|---|---|---|---|---|---|
| | | | Electron-Rich Region[b] | | |
| $NH_3$ | −0.083 | −0.075 | −0.137 | −0.089 | −0.078 |
| $H_2O$ | −0.065 (57°) | −0.079 (0°) | −0.098 (57°) | −0.075 (15°) | −0.076 (0) |
| HF | −0.041 (30°) | −0.065 (0°) | −0.061 (60°) | −0.061 (0°) | −0.059 (0) |
| $PH_2$ | 0.002 | −0.019 | −0.088 | −0.034 | −0.016 |
| $H_2S$ | −0.040 (>90°) | −0.026 (0°) | −0.056 (65°) | −0.026 (50°) | −0.024 (0) |
| HCl | −0.021 (>90°) | −0.024 (0°) | −0.029 (70°) | −0.021 (0°) | −0.022 (0) |
| | | | Electron-Poor Region[d] | | |
| $NH_3$ | 0.044 | 0.019 | 0.020 | 0.020 | 0.023 |
| $H_2O$ | 0.061 | 0.037 | 0.039 | 0.038 | 0.041 |
| HF | 0.085 | 0.060 | 0.061 | 0.060 | 0.065 |
| $PH_3$ | 0.041 | 0.004 | 0.003 | 0.004 | 0.008 |
| $H_2S$ | 0.056 | 0.016 | 0.018 | 0.017 | 0.019 |
| HCl | 0.075 | 0.031 | 0.032 | 0.032 | 0.034 |

[a] Units are au/Å. [b] Electrostatic potential at 2.12 Å for $NH_3$, $H_2O$, and HF and 2.65 Å for $H_3P$, $H_2S$, and HCl (see ref 1 and 2); in parentheses is angle from dipolar axis where optimum (most negative) electrostatic potential occurs. [c] See Figure 1 for an explicit representation of these five types of charge distribution for $H_2O$. [d] Electrostatic potential at 2 Å along A–H axis.

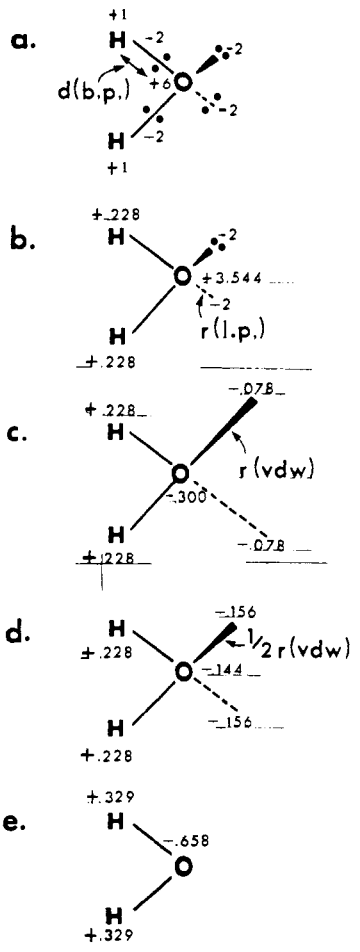


Figure 1. (a) Two-electron bond pair and lone pair representation of water; see Table I for detailed locations of charges. (b) Partial charge bond pair and two-electron lone pair representation of $H_2O$. (c) Partial charge bond pair and partial charge lone pair representation of $H_2O$; lone pairs at van der Waals radius. (d) As in (c), but lone pairs at ½ van der Waals radius. (e) Atom centered partial charge representation of water.

above-described charge distribution are to locate the lone pairs at the van der Waals radii (c) or at ½ the van der Waals radius[15] (d) rather than so close to the nucleus. This merely involves a change in $d$(lp) and the use of partial negative charges (rather than −2 charges) at the van der Waals radius and corresponding partial positive charges at the atom to reproduce $\mu$(lp). A fourth choice might be to use only atom-centered partial charges (e) such that the molecular dipole moment is reproduced. We illustrate these charge distributions for $H_2O$ in Figure 1.[16]

We next evaluated the electrostatic potential for these charge distributions and the results, using our previously described "reference positions",[17] are described in Table II.

The partial charge representations more closely follows the relative electrostatic potential and its angular dependence found in quantum mechanical calculations.[1,2] We decided to subject these charge distributions to a more rigorous test and evaluated the energy of the water dimer, keeping the O–O distance fixed at 3.0 Å and allowing the remaining five intermolecular coordinates to vary. As one can see from Figure 2, the partial charge representations (c) and (d) most closely reproduce the observed H bond geometry—near linear H bond with $\theta \sim$ ½ the tetrahedral angle. Charge distributions of type (c) for the six hydrides are shown in Figure 3.

Because it is easy to evaluate the energy and geometry of dimer formation with such an approach, we did so for the 36 dimers we studied previously with quantum mechanical methods.[1] Table III contains the results for the partial charge representation with line pair at van der Waals radius (see Figure 3); Table IV, the corresponding results using the partial charge lone pair at ½ van der Waals radius (½ vdW). A comparison with quantum mechanical surfaces[1,2] shows generally good agreement for geometries (near linear H bonds) but the interaction energies are very different for the two types of charge distributions. The magnitudes of the ½ vdW partial charge energies are in better agreement with the best ab initio calculations, but incorrectly predict that $(HF)_2$ and $(HCl)_2$ will be linear. The interaction energies of the second row dimers (HCl, $H_2S$, and $PH_3$) are generally underestimated, comparing their relative energies with the first-row dimers. This is consistent with the observation that charge redistribution effects play a much larger role in stabilizing the second-row dimers.[1,2] In particular HCl is predicted to be a much weaker proton donor than $H_2O$, whereas for relatively strong Lewis bases, the two are apparently competitive in the gas phase (at the 431G level, $H_3N\cdots HCl$ is bound more tightly than $H_3N\cdots HOH$).[1] The ½ vdW representation correctly finds,[18] as did the 431G calculations, that HF···HCl is more stable than HCl···HF, whereas the vdW representation predicts the latter to be slightly (3.10 vs. 3.00 kcal/mol) more stable.

Another possible way to compare the derived charge distributions is to compare the quadrupole moments with those calculated with very accurate wave functions. This is possible

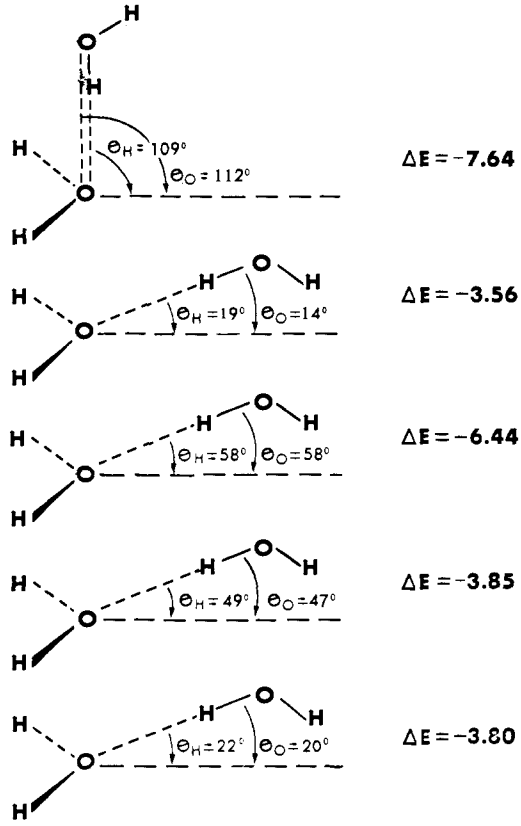


**Figure 2.** Water dimer surfaces for the five charge distributions described in Figure 1; $R$(O–O) = 3.0 Å. $\theta_H$ is angle between H···O bond and dipolar axis of proton acceptor; $\theta_O$ is angle between O···O bond and dipolar axis of proton acceptor. $\Delta E$ are in kcal/mol.

for $H_2O$, but for larger molecules, the quadrupole moment and its component are often unavailable. Table V has such a comparison for $H_2O$. As one can see, there is a large variation in the calculated $\theta_{ij}$'s but none is in very good agreement with experiment and the magnitude of the quadrupole moment does not correlate very well with the calculated interaction energies (Figure 2).

$PH_3$ is a very interesting case where the A–H dipole moment is negative $A^{\delta+}$–$H^{\delta-}$, and the observed direction of the dipole moment comes from the lone pair moment, which is larger than the bond moments and of the opposite sign. With the simple charge model this molecule is correctly predicted to be a moderately good Lewis base, better than $H_2S$ and HCl, but weaker than HF, $H_2O$, and $NH_3$.[19] However, as a Lewis acid, our simple calculations (Tables III and IV) find it to not form P–H···B bonds, but rather bifurcated bonds or to line up in "trifurcated" fashion, e.g.,

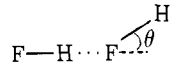

It is interesting to note that all the electronegativity scales place H above P, but by varying amounts. However, the sign of the P–H bond moment or the quantitative accuracy of our eq 1 has not been carefully analyzed by quantum mechanical methods. With the charge distributions described above, P–H···B bonds are not really H bonds, because unlike the remaining proton donors in Tables III and IV, they do not form *near* linear A–H···B bonds in the most stable structure. We note that the electrostatic potential and its gradient do not have their maximum (at 2 Å from the proton) exactly along the A–H axis for $H_2O$, $H_2S$, or $HNH_2$, but do for HF and HCl (Table VI). For the first three, the maximum electrostatic potential gradient occurs only slightly (~10–15°) off axis, whereas for $PH_3$ this maximum occurs along the threefold axis.

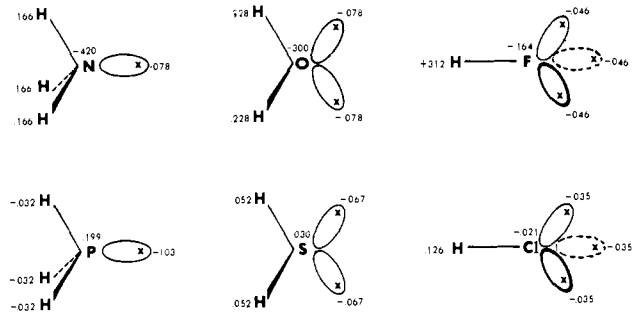

**Figure 3.** Charge representation of the hydrides; partial charge bond pair, lone pair at van der Waals radius.

**Table III.** Hydride Dimer Interaction Energies and Geometries Charge Representation (c)

| Proton donor[a] | Electron donor HF | $H_2O$ | $H_3N$ | HCl | $H_2S$ | $H_3P$ |
|---|---|---|---|---|---|---|
| FH | | | | | | |
| $-\Delta E$[b] | 7.05 | 12.85 | 18.41 | 3.10 | 6.31 | 10.38 |
| $\theta_A$[c] | 60.0 | 57.3 | 0.0 | 70.3 | 64.6 | 0.0 |
| $\theta_H$[d] | 58.6 | 56.6 | 0.0 | 69.3 | 64.3 | 0.0 |
| HOH | | | | | | |
| $-\Delta E$ | 3.86 | 6.44 | 8.22 | 1.44 | 2.63 | 3.93 |
| $\theta_A$ | 59.9 | 57.5 | 0.5 | 71.4 | 65.6 | 1.2 |
| $\theta_H$ | 59.4 | 57.5 | 1.1 | 70.9 | 65.8 | 1.5 |
| $H_2NH$ | | | | | | |
| $-\Delta E$ | 1.89 | 2.96 | 3.52 | 0.63 | 1.03 | 1.45 |
| $\theta_A$ | 63.6 | 59.0 | 1.2 | 76.0 | 67.4 | 2.3 |
| $\theta_H$ | 61.6 | 58.4 | 2.0 | 74.0 | 67.3 | 2.7 |
| ClH | | | | | | |
| $-\Delta E$ | 3.00 | 5.31 | 7.45 | 0.95 | 1.81 | 2.83 |
| $\theta_A$ | 59.0 | 56.9 | 0.00 | 69.6 | 64.5 | 0.0 |
| $\theta_H$ | 57.5 | 56.2 | 0.0 | 68.0 | 63.9 | 0.0 |
| HSH | | | | | | |
| $-\Delta E$ | 1.01 | 1.56 | 1.88 | 0.35 | 0.60 | 0.82 |
| $\theta_A$ | 54.0 | 54.9 | 1.4 | 68.6 | 65.1 | 1.8 |
| $\theta_H$ | 54.8 | 55.5 | 2.3 | 68.5 | 65.6 | 2.5 |
| $H_2PH$ | | | | | | |
| $-\Delta E$ | (0.16) | (0.20) | (0.25) | (0.25) | 0.04) | (0.13) |
| $\mu_A$[e] $\theta_H$[e] | 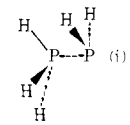 (i) | | | | | |

[a] We used the following distances, based on the best available experiments and theory.[1,2] For proton donors: F–H, $R$ = 2.8 Å for first row electron donors, $R$ = 3.4 Å for second row; O–H, $R$ = 3.0 Å (first row); 3.7 Å (second); $HNH_2$, $R$ = 3.2 Å (first row), $R$ = 4.0 Å (second); HCl, $R$ = 3.2 Å (first), $R$ = 4.0 Å (second); HSH, $R$ = 3.6 Å (first), $R$ = 4.4 Å (second); $HPH_2$, $R$ = 4.1 Å (first), $R$ = 4.8 Å (second). See ref 1 for a justification of using a constant $R$ for a given A–H bond and all B of same row. [b] Interaction energy in kcal/mol. [c] Angle between B···A bond and dipolar axis of electron donor. [d] Angle between B···H bond and dipolar axis of electron donor. [e] For $HPH_2$ as proton donor, there appeared to be no local minimum in the B···H–P surface; the molecules moved to make $PH_3$ the electron donor, therefore, we constrained this search to the part of the surface where $PH_3$ was facing the electronegative end of the electron donor. The molecules minimized at a geometry which was either trifurcated (i) ($PH_3$, HF, $H_2O$, $NH_3$) as electron donors or highly distorted from a linear A–H···B bond ($H_2S$ and HCl as electron donors).

We have compared the 431G energy for $H_3P$···$HPH_2$, $R$(P–P) = 4.8 Å, for the linear and trifurcated geometries and find the linear more stable ($-\Delta E$ = 0.8 kcal/mol) compared to the trifurcated ($-\Delta E$ = 0.5 kcal/mol). It is not clear at this stage how accurate these calculations are because this basis set is still somewhat limited and one expects a ~0.5–1 kcal/mol counterpoise correction for this interaction.[1,2,22] If more ac-

Table IV. Hydride Dimer Interaction Energies and Geometries Charge Representation (d)

| Proton donor[a] | Electron donor HF | $H_2O$ | $H_3N$ | HCl | $H_2S$ | $H_3P$ |
|---|---|---|---|---|---|---|
| FH | | | | | | |
| $-\Delta E$[b] | 4.56 | 6.46 | 8.20 | 1.33 | 2.04 | 2.80 |
| $\theta_A$[c] | 0.0 | 45.1 | 0.0 | 59.1 | 60.6 | 0.0 |
| $\theta_H$[d] | 0.0 | 43.3 | 0.0 | 56.1 | 59.0 | 0.0 |
| HOH | | | | | | |
| $-\Delta E$ | 2.76 | 3.85 | 4.37 | 0.80 | 1.12 | 1.33 |
| $\theta_A$ | 39.0 | 47.2 | 6.0 | 61.7 | 61.8 | 4.5 |
| $\theta_H$ | 41.3 | 48.9 | 8.4 | 62.6 | 63.5 | 6.9 |
| $H_2NH$ | | | | | | |
| $-\Delta E$ | 1.42 | 1.89 | 2.05 | (0.41)[e] | 0.52 | 0.56 |
| $\theta_A$ | 64.1 | 55.8 | 12.0 | (76.0) | 69.6 | 7.9 |
| $\theta_H$ | 61.4 | 56.1 | 14.0 | (74.0) | 70.0 | 10.4 |
| ClH | | | | | | |
| $-\Delta E$ | 2.20 | 2.98 | 3.75 | 0.53 | 0.76 | 1.01 |
| $\theta_A$ | 0.0 | 41.1 | 0.0 | 50.9 | 57.8 | 0.0 |
| $\theta_H$ | 0.0 | 39.3 | 0.0 | 47.9 | 55.9 | 0.0 |
| HSH | | | | | | |
| $-\Delta E$ | 0.91 | 1.19 | 1.31 | 0.26 | 0.34 | 0.38 |
| $\theta_A$ | 20.8 | 34.1 | 6.3 | 40.6 | 55.5 | 4.5 |
| $\theta_H$ | 27.1 | 38.7 | 10.1 | 46.5 | 58.9 | 8.6 |
| $H_2PH$ | | | | | | |
| $-\Delta E$[f] | 0.24 | 0.29 | 0.31 | 0.09 | 0.10 | 0.11 |
| $\theta_A$ | | | | | | |
| $\theta_H$ | | | | | | |

[a] See Table III, footnote *a*, for choice of *R*. [b] See Table III, footnote *b*. [c] See Table III, footnote *c*. [d] See Table III, footnote *d*. [e] This surface had to be constrained. [f] See footnote *e*, Table III; all but $H_2S\cdots HPH_2$ were trifurcated, and $H_2S\cdots HPH_2$ was halfway between S···H–P and trifurcated.

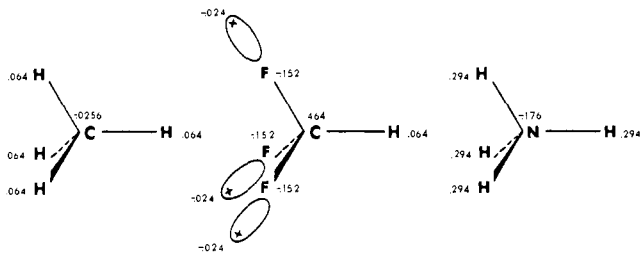


Figure 4. Representation of $CH_4$, $NH_5^+$, and $CF_3H$, partial charge bond pair, lone pair at van der Waals radius. For $CF_3H$, we have projected the lone pairs along the CF axis (each has a charge of −0.008).

curate calculations confirm our sign of the P–H dipole moment and the structure of $(PH_3)_2$ turns out to be *linear*, this may be an interesting H-bonded case where charge transfer effects have a *qualitatively* significant effect and outweigh the tendency expected from electrostatics alone.

### The Electrostatic Potential for Charge Distributions in Other Molecules

We now proceed to develop representations of the charge distributions in a number of other molecules and compare the electrostatic potentials determined with such representations with the electrostatic potentials found in quantum mechanical calculations, using experimental monomer geometries (Table VII) and the van der Waals representation.

**A. $CH_4$, $NH_4^+$, $Li^+$, $F^-$, $CH_3F$, $CH_3OH$, $CH_3NH_2$, and $CF_3H$.** The extension of method of deriving the charge distribution in $CH_4$ and $NH_4^+$ is straightforward (Figure 4); we derive bond moments according to eq 1 and, in the case of $NH_4^+$, divide the +1 charge proportionately to the electronegativity to ensure a net +1 charge. Based on simple analyses we have done, $Li^+$ and $F^-$ can be satisfactorily represented by full charges centered at the atom, although for the latter, an explicit representation of the lone pairs as in H–F ($r$(lp) = 1.35 Å, $q$(lp) = −0.046) is also reasonable.

Table V. Calculated Quadrupole Moment Components[a] for Charge Representations[a]

| Charge representation | $\theta_{XX}$ | $\theta_{YY}$ | $\theta_{ZZ}$ |
|---|---|---|---|
| (a) | −2.83 | 3.02 | −0.19 |
| (b) | −0.81 | 1.13 | −0.32 |
| (c) | −1.69 | 1.75 | −0.05 |
| (d) | −1.28 | 1.38 | −0.10 |
| (e) | −1.31 | 2.63 | −0.13 |
| Experiment[b] | −2.50 | 2.63 | −0.13 |

[a] esu Å$^2$ = buckinghams; relative to center of mass for $H_2O$,[16] see Figure 1 for these. [b] See ref 20 for an extensive comparison of accurate quantum mechanically calculated $\theta$'s and experimental values.

Table VI. Electrostatic Potential and Its Gradient as a Function of Angle off the A–H Axis

| Molecule | ESPOT[a] | $\theta$[b] | $\nabla$(ESPOT)[c] | $\theta$[b] |
|---|---|---|---|---|
| FH | 0.061 | 0 | −0.029 | 0 |
| HOH | 0.042 | 30 | −0.020 | 10 |
| $H_2NH$ | 0.023 | 30 | −0.011 | 10 |
| ClH | 0.032 | 0 | −0.015 | 0 |
| HSH | 0.019 | 20 | −0.008 | 10 |
| $H_2PH$ | 0.006 | 57 | −0.002 | 57 |

[a] Electrostatic potential at $R$ = (2.0 + $r$(A–H)) Å. Units are au/Å, van der Waals representation (c). [b] Angle relative to A–H direction of maximum in electrostatic potential or gradient at $R$. [c] *Finite* gradient in electrostatic potential $\nabla$(ESPOT) = ESPOT($R$) − ESPOT($R$ + 1). Units are au/Å$^2$.

Using these charge distributions, the electrostatic potentials near these molecules have been determined and the results are in good qualitative agreement with those found in quantum mechanical calculations.

One can use this algorithm to construct the charge distribution of $CH_3$–F, $CH_3$–OH, and $CH_3$–$NH_2$ merely transferring the charge distributions of $CH_4$, HF, $H_2O$, and $NH_3$ and using the electronegativities to determine the C–X bond moment. Such charge distributions correctly predict that $\mu(CH_3F) > \mu(HF)$ ($\mu(CH_3F)_{calcd}$ = 1.95; $\mu(CH_3F)_{exp}$ = 1.85), but find too large dipole moments for $CH_3OH$ ($\mu_{calcd}$ = 1.90, $\mu_{exp}$ = 1.70) and $CH_3NH_2$ ($\mu_{calcd}$ = 1.64, $\mu_{exp}$ = 1.30). The question one might address is: how can one change the charge distribution to bring it in line with the experimental dipole moment?

We considered a number of possible changes in the charge distributions, and the one which seemed to give the most reasonable agreement with the quantum mechanical "methyl substituent effect"[23] on the electrostatic potential in the lone pair region in these molecules is to change the C–$H_3$ dipole moment to force the methyl-substituted molecules to have the correct dipole moment. This is illustrated in Figure 5 and the electrostatic potentials are reported in Table VII. This charge alteration was not successful in reproducing the fact that the quantum mechanically calculated electrostatic potential (ESPOT) was greater for $CH_3F$ than HF, but did find ESPOT($CH_3B$) < ESPOT(HB) for B = OH and $NH_2$.

Earlier[1] it was noted that the significantly improved proton donating ability of $CF_3H$ relative to $CH_4$ could be rationalized with their relative electrostatic potentials. We thus constructed a charge distribution for $CF_3H$, using the above-described algorithm. This had a dipole moment of 2.40 D; to bring the molecular dipole into agreement with experiment, we changed the F lone pair moments appropriately and the resulting electrostatic potential (see Figure 4) for this charge distribution

**Table VII.** Comparison of Electrostatic Potentials Calculated with Simple Charge Representations and Those Calculated Quantum Mechanically

| Electronegative Regions | | | | | Electropositive Regions[p] | | | | |
|---|---|---|---|---|---|---|---|---|---|
| Molecule | Simple ESPOT[a] | $\theta$[b] | Q.M. ESPOT[a] | $\theta$[b] | Molecule | Simple ESPOT | $\theta$[q] | Q.M. ESPOT | $\theta$ |
| $H_3N$ | −0.137 | 0 | −0.141 | 0 | F-H | 0.061 | 0 | 0.083 | (0) |
| $H_2O$ | −0.098 | 57[c] | −0.112 | 0[c] | HO-H | 0.039 | (0) | 0.057 | (0) |
| HF | −0.061 | 60 | −0.068 | 0 | $H_2N$-H | 0.020 | (0) | 0.032 | (0) |
| $H_3P$ | −0.088 | 0 | −0.055 | 0 | Cl-H | 0.032 | 0 | 0.064 | (0) |
| $H_2S$ | −0.056 | 65[c] | −0.049 | 45[c] | HS-H | 0.018 | (0) | 0.036 | (0) |
| HCl | −0.029 | 70 | −0.030 | 45 | $H_2P$-H | 0.003 | (0) | 0.009 | (0) |
| $F^-$ | −0.473 | | −0.473 | | $H_3C$-H | 0.002 | 0 | 0.006 | (0) |
| $F_2$[d] | −0.003 | 75° and $\pi$[e] | −0.005 | 85°[c] | $F_3C$-H | 0.046 | (0) | 0.068 | (0) |
| | | | | | NC-H | 0.051 | 0 | 0.074 | (0) |
| $H_2$[d] | −0.002 | $\pi$[f] | −0.001 | $\pi$[f] | CN-H | 0.056 | 0 | 0.072 | (0) |
| $N_2$[d] | −0.020 | 0 | −0.008 | 0 | CHOHNH | 0.050 | (0) | 0.078 | (0) |
| | | | | | | (0.010) | | (0.042) | |
| HCN | −0.106 | 0 | −0.095 | 0 | $O_2S$ | 0.046 | 70°[r] | 0.072 | 75°[r] |
| HNC | −0.093 | 0 | −0.089 | 0 | $O_2C$ | 0.027 | $\pi$[s] | 0.038 | $\pi$[s] |
| $H_2CO$ | −0.084 | 60[g] | −0.093 | 0 | $H_2$ | 0.005 | 0[t] | 0.003 | 0[t] |
| $H_2CO$ (n→$\pi$*) | −0.021 | $\pi$(C)[h] | | | $F_2$ | 0.006 | 0[t] | 0.002 | 0[t] |
| | | | | | $N_2$ | 0.010 | $\pi$[u] | 0.006 | $\pi$[u] |
| $H_2CO$ ($\pi$→$\theta$*) | −0.070 | 60[g] | | | $H_3N^+$-H | 0.342 | (0) | 0.348 | (0) |
| $H_2NCHO$[i] | −0.110 | lp trans[j] | −0.112 | lp trans[j] | $Li^+$ | 0.500 | v | 0.500 | l |
| $H_2NCHO$ | −0.107 | lp cis[k] | −0.083 | lp cis[k] | | | | | |
| $H_2NCHO$ | −0.035 | $\pi$ − O[l] | −0.060 | $\pi$ − O[l] | | | | | |
| $CH_3NH_2$[m] | −0.130 | (0) | −0.134 | 0 | | | | | |
| $CH_3OH$[m] | −0.097 | (57) | −0.108 | 0 | | | | | |
| $CH_2F$[m] | −0.060 | (60) | −0.071 | 0 | | | | | |
| $C_2H_4$ | −0.018 | n | −0.049 | n | | | | | |
| $C_2H_2$ | −0.010 | n | −0.030 | n | | | | | |
| $SO_2$ | −0.067 | lp[o] | −0.076 | lp[o] | | | | | |
| $CO_2$ | −0.040 | 60 | −0.045 | 0 | | | | | |

[a] ESPOT = electrostatic potential at 2.12 Å from C, N, O, or F; 2.65 Å from S, Cl, or P unless otherwise specified; units are au/Å, charge representation (c) used for simple ESPOT. [b] Angle of minimum ESPOT relative to dipolar axis. [c] Angle is out of plane angle relative to dipolar axis. [d] $F_2$, $N_2$, and $H_2$ were examined at 2.65 Å from the atom to be consistent with the minimum energy distances found in ref 2. [e] The simple ESPOT had two minima, one at 75° relative to the F-F axis and one ⊥ and bisecting the F-F bond ($\pi$). [f] Minimum potential ⊥ to the H-H bond and bisecting it. [g] Angle in plane relative to C=O axis. [h] Minimum ESPOT is ⊥ to $H_2CO$ plane and over carbon. [i] See D. M. Hayes and P. Kollman, *J. Am. Chem. Soc.*, **98**, 3335 (1976), for exact location; we used a planar formamide model in this study. [j] Lone pair cis to CN bond ($\theta$ = 60° relative to C=O). [k] Lone pair cis to CN bond ($\theta$ = 60° relative to C=O). [l] Perpendicular to molecular plane. [m] Evaluated ESPOT at the minimum $\theta$ found in the calculations on the corresponding hydride. [n] Above center of $\pi$ bond. [o] Along oxygen lone pair ~ parallel to dipolar axis. [p] Electrostatic potential at 2 Å from H, unless otherwise specified. [q] Assumed along X-H bond, unless otherwise specified (see Table VI). [r] Relative to $SO_2$ dipolar axis, out of plane angle at 2.65 Å. [s] $\pi$ to molecular axis—"above" the carbon at 2.65 Å; see ref 2 for rationale of this choice of *R*. [t] Along bond axis at 5 au (2.65 Å) from H, N, or F. [u] $\pi$ to $N_2$ axis, above center of bond. [v] At 2 Å from $Li^+$.

is reported in Table VII. As one can see, the electrostatic potential difference between $CH_4$ and $CF_3H$ is qualitatively similar for both the quantum mechanically calculated and our simple charge distribution.

**B. Extension to Differently Hybridized and $\pi$ Bonded Systems: $H_2CO$, HCN, HNC, $C_2H_4$, $C_2H_2$.** Next one considers the extension of this approach to systems with differently hybridized lone pairs and with $\pi$ bonds. We first focus our attention on $H_2CO$. Where do we place the lone pairs in this molecule? We expect that a pure s lone pair will be spherically symmetric, so the asymmetry of the line pair should be proportional to the "p" character. We thus take the line pairs of $H_2O$ and reduce their distance from the O by $^2/_3/^3/_4$, the ratio of p characters. The C-H and C-O bonds are chosen as before (eq 1), and this leaves the C-O $\pi$ bond. To a first approximation, we will ignore the out of plane "extent" of the $\pi$ bond and use the partial charge representation of it as well. We place an appropriate partial charge at the C and O so that the molecule has the correct (2.34 D) dipole moment. This leads to the charge distribution shown in Figure 6. A similar approach to the charges in HCN and HNC (now scaling the lone pair length by $^1/_2/^3/_4$), leads to their charge distributions in Figure 7. Finally, a simple charge distribution of $C_2H_4$ and $C_2H_2$ is illustrated in Figures 6 and 7. A comparison of the calculated electrostatic potentials for these molecules with the quantum mechanically calculated values is in Table VII. As one can see, the agreement is qualitatively satisfactory.

**C. Extension to Excited States and Molecules with Resonance Structures—$H_2NCHO$, $H_2CO$ (n→$\pi$*), $H_2CO$ ($\pi$→$\pi$*).** The charge distribution of formamide can be constructed from the fragments $NH_3$ and $H_2CO$, but such a choice leads to far too small a dipole moment for the molecule. Thus, an appropriate amount of N → O charge transfer was carried out in order to reproduce the experimental dipole moment. In this way, one is representing the contribution of the $^+N{=}C{-}O^-$ resonance structure to the overall wave function. This charge distribution is shown in Figure 7 and the electrostatic potential is compared with a quantum mechanically calculated one in Table VII.

How can one predict the charge distribution of excited states? A qualitative knowledge of the nature of the ground and excited state molecular orbitals allows this. First, we transform our partial charge representation of $H_2CO$ back into electron pair terms. If the $\pi$ orbital has the electronic structure $\pi = C_1\, 2p_\pi(C) + C_2\, 2p_\pi(O)$, then the $\pi^*$ will be of the form $\pi^* = C_2\, 2p_\pi(C) - C_1\, 2p_\pi(O)$ and will have approximately the

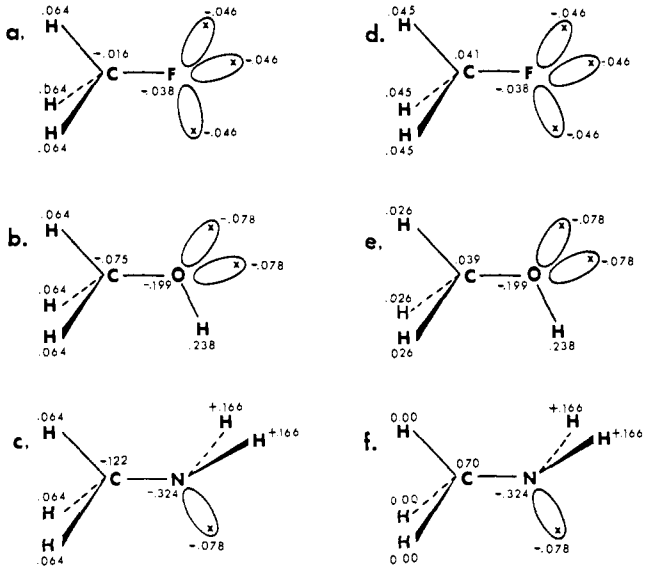

Figure 5. Charge representations of $CH_3F$, $CH_3OH$, and $CH_3NH_2$. (a), (b), and (c) are constructed using the hydride algorithm; (d), (e), and (f) are the charge distributions altered in the C–$H_3$ dipole so that the molecular dipole moment is in agreement with experiment. Partial charge bond pair, lone pairs at van der Waals radius.

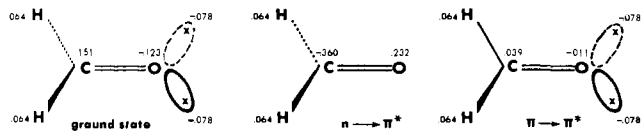


Figure 6. Charge representations of $H_2CO$ ground, n→π*, and π→π* states; partial charge bond pair, lone pair at van der Waals radius.

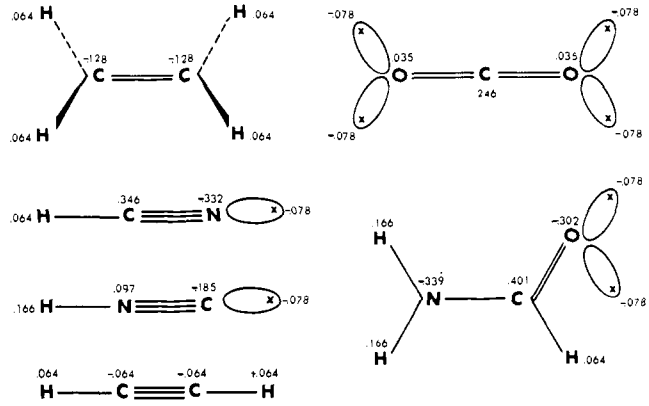

Figure 7. Charge representations of $C_2H_2$, $C_2H_4$, $H_2NCHO$, HCN, HNC, and $CO_2$; partial charge bond pair, lone pair at van der Waals radius.

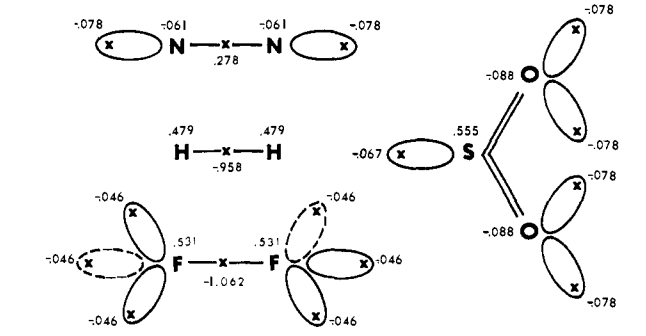

Figure 8. Charge representations of $H_2$, $F_2$, $N_2$, and $SO_2$; partial charge bond pair, lone pair at van der Waals radius.

*opposite* sign bond dipole. A similar analysis for the n→π* state leads to the vanishing of the lone pair dipole and the charge distributions shown in Figure 6. A comparison of the partial charges for these states with those found quantum mechanically is given in Table VIII. The fact that the oxygen in $H_2CO$ (n→π*) has little H-bond acceptor ability and the carbon in both excited states is a better H-bond base than in the ground state is qualitatively rationalized by our derived charge distributions and corresponding electrostatic potentials (Table VII). Comparing the electrostatic potential for $H_2CO$ (n→π*) and the $H_2CO$ ground state leads one to expect the n→π* state to have its most basic site above the C and be able to form a C···H–O hydrogen bond to water about 1/4 as strong as the C=O···HOH hydrogen bond in ground-state $H_2CO$. This is consistent with the quantum mechanical calculations of Iwata and Morokuma.[24]

**D. Charge Distributions in Some Other Simple Molecules: $SO_2$, $H_2$, $N_2$, and $CO_2$.** We can see the above-described approach to construct a charge distribution for $SO_2$ (varying the S–O π bond moment to fit the molecular dipole moment and taking the O $sp^2$ lone pairs from $H_2CO$) and some nondipolar molecules. $H_2$ is a special problem because there is no way to reproduce the experimental *quadrupole* moment without placing some charge on the bond axis. An analysis of $N_2$ and $F_2$ (placing lone pairs in the same manner as described above: sp lone pairs for $N_2$ and $sp^3$ lone pairs as in HF for $F_2$) suggests that a partial charge in the center of the bond is required to reproduce the experimental quadrupole moment. Similarly, $CO_2$ appears to have a smaller C=O bond dipole than one would predict, constructing this molecule from two formaldehyde-"like" C=O groups. So, for these nondipolar molecules, we used experimental quadrupole moments to fix the magnitude of the charges along the bond axis. The derived charge distributions for these molecules are illustrated in Figure 7 and the description of the electrostatic potential around these molecules is given in Table VII. Once again, the agreement with quantum mechanical calculation is qualitatively satisfactory, and with the experimental observations of $(N_2)_2$ as T-shaped and $(Cl_2)_2$ as apparently "L"-shaped (see Figures 7 and 8).

**Table VIII.** Comparison of Partial Charges for $H_2CO$ (Ground State), $H_2CO$ (n→π*), and $H_2CO$ ($^3$π→π*)

| Simple representation[a] | | Quantum mechanical[b] |
|---|---|---|
| Ground state | | |
| C | 0.151 | +0.150 |
| O | −0.279 | −0.190 |
| H | 0.064 | +0.020 |
| $^3$n→π* | | |
| C | −0.360 | −0.380 |
| O | 0.232 | +0.200 |
| H | 0.064 | +0.090 |
| $^3$π→π* | | |
| C | 0.039 | 0.080 |
| O | −0.167 | −0.110 |
| H | 0.064 | 0.020 |

[a] Lone pairs included as part of oxygen population. [b] See ref 25. The corresponding singlet states have approximately the same populations. The actual minimum energy geometry for the n→π* state is bent, but we are using the planar results of ref 20 for comparison.

**E. Comparison of ESPOT from Simple and Quantum Mechanical Charge Distributions.** In general, the agreement with quantum mechanical calculations (Table VII) is qualitatively satisfactory, with the magnitude of ESPOT in the electronegative regions comparable, but about 1/2 too small in the electropositive regions. Interesting exceptions are $C_2H_2$ and

$C_2H_4$; there, the atom-centered ESPOT is substantially smaller in magnitude than the quantum mechanical. This might be remedied by representing the $\pi$ electrons explicitly, perhaps letting them extend from the atom about $\frac{1}{2}$ as far as the lone pairs. The quantum mechanical potentials are expected to be too large, since the 431-G basis employed in ref 1 and 2 exaggerates dipole moments. It may be that eq 1 underestimates bond moments and, thus, somewhat overestimates lone pair moments. A subsequent analysis might use very accurate calculations on the hydrides to alter eq 1 to try to reproduce ESPOT for these hydrides, and then use such an algorithm on the remaining molecules.

In summary, we have presented a simple algorithm for representing the charge distribution of molecules: (a) use eq 1 to locate bond pairs; (b) use observed dipole moments and the hybridization of the lone pair orbitals to locate the lone pairs; (c) locate $\pi$ electron pairs by forcing molecules to have the correct dipole moment; (d) use transferable bond pairs, lone pairs, and $\pi$ bonds to build up larger molecules, modifying them (as described for formamide, $CH_3NH_2$, and $H_2$) to reproduce the observed molecular electrostatic moments. The above description allows one to use either a partial charge or full charge representation of the bond pairs and lone pairs, but our results suggest that the partial charge representations (c) and (d) are the most realistic.

### Uses of Simple Charge Representations and a Physical Basis for This Approach

The charge distributions presented here might be used directly in empirical potential function approaches such as those developed by Spears.[25] For example, in comparing $NH_3$ vs. HCN as Lewis bases, it is crucial that a more sophisticated (not just point dipole) representation of the molecular charge distributions be employed. The charge distributions employed here are preferable to Mulliken population analyses from most quantum mechanical calculations because (1) they use explicit lone pair representations and (2) all but the most accurate quantum mechanical calculations do not accurately reproduce the molecular dipole moment.

Eventually, we hope to incorporate these ideas about charge distributions into empirical potentials which contain the other important energy terms. But already at this stage we can use them in a qualitative way to predict the strength and directionality of intermolecular interactions. Previously,[2] we have noted that the electrostatic potentials for Lewis acids and bases can be related to the quantum mechanically calculated intermolecular interaction energy by the empirical equation

$$\Delta E = 1123 \times \mathrm{POTA} \times \mathrm{POTB} \qquad (2)$$

where $\Delta E$ is in kcal/mol and POTA and POTB are in au/Å. We now use the electrostatic potentials determined from the charge distributions we derived above (Table VII) together with an assumed $(H_2O)_2$ dimerization energy ($\Delta E = -5.3$ kcal/mol) to derive a similar relationship for the simple charge representation.

$$\Delta E = 1390 \times \mathrm{POTA} \times \mathrm{POTB} \qquad (3)$$

The use of the electrostatic potential as in eq 2 and 3 is a way of modeling not just the electrostatic effects, but also charge redistribution and exchange repulsion energies. For example, if an acid feels a more negative electrostatic potential from an upcoming base, it will have a greater electrostatic attraction for this base, but also polarize more (polarization energy) and allow more charge transfer. We feel that the use of the electrostatic potential in eq 2 and 3 allows one to "predict" many aspects of the structure and energies of intermolecular complexes. However, there are alternate ways of looking at the Lewis acid-Lewis base interactions. For example, the above relationships (eq 2 and 3) can be compared with that suggested by Mulliken[8] for charge transfer complexes:

$$\Delta E \propto \frac{\text{electron affinity (electron acceptor)}}{\text{ionization potential (electron donor)}} \qquad (4)$$

and that suggested that by Allen for H bonds[9]

$$\Delta E \propto \frac{\text{bond dipole (proton donor)}}{\text{ionization potential relative to nearest rare gas (electron donor)}} \qquad (5)$$

The latter two have the advantage that they are simpler and it is often easier to derive part of the right-hand side from experiments. Our equation has the advantage that it is a more general relationship and can be used to examine directionality of the interactions and excited states in a more straightforward and more precise way. Most moderate and weak intermolecular interactions are dominated by the electrostatic energy and our approach takes advantage of this finding. It also allows straightforward consideration of "long-range" effects as well as the specific A···:B interaction in considering intermolecular interactions. Del Bene has noted[26] that H bonds are often characterized by the approach of an A-H bond toward a hybridized B: lone pair, but often long-range "dipole-dipole" interactions cause deviations from this idealized geometry. The use of the electrostatic potential allows one to evaluate both of the forces in a single calculation and incorporate them in a straightforward way in predicting interaction energies and geometries (eq 3).

However, it should be emphasized that eq 2-5 are similar ways of looking at the same phenomena.[27] A "better" Lewis base has a line pair more available for donation (lower ionization potential and greater electrostatic potential) and a "better" Lewis acid has a greater more available vacant orbital (lower LUMO or more positive electrostatic potential). Equations 2 and 3 require the choice of a reference point for the electrostatic potential; eq 4 and 5 require, e.g., for first row-second row comparisons, a scaling of ionization potentials to the corresponding noble gas. Equation 4 also requires a separation of bond dipoles from other dipoles.

### Caveats in the Application of Equation 3

**A. Electrostatic Potential vs. Electrostatic Potential Gradient.** Earlier we have pointed out that for interactions between dipolar molecules,[2] the *electrostatic potential gradient* is a more precise predictor of relative interaction energies and geometries than the electrostatic potential. For example, a Lewis base B will interact attractively with the H and repulsively with the A of a Lewis acid $A^-H^+$ and thus the larger (more negative) the electrostatic potential gradient due to B, the larger the net A-H···B attraction. We thus compared the strength and directionality of the electrostatic potential gradient with that obtained quantum mechanically and the results are given in Table IX for the six hydrides, HF, $H_2O$, $NH_3$, HCl, $H_2S$, and $PH_3$. As one can see, the order of basicity and acidity is the same whether one uses the electrostatic potential or its gradient as a measure. However, we should emphasize again that there is a significant difference between the way the two different simple representations interleave the relative first and second row base strengths; also, both underestimate the acid strength of H-Cl.

We have shown,[2] using the quantum mechanical charge distributions, that there are situations (e.g., $\Delta E$(HCN···HF) vs. $\Delta E$(HNC···HF)) where the electrostatic potential gradient correctly predicts the relative order, but the electrostatic potential does not. Thus, especially in case of small and subtle differences, the gradient is more reliable than the potential and is worth examining.

Table X contains the electrostatic potential gradients for

**Table IX.** Comparison of Electrostatic Potential Gradients for the Simple Charge Distribution and the Quantum Mechanically Calculated Distributions

| Molecule | Simple ∇(ESPOT)[a] (c)[c] | Simple ∇(ESPOT)[a] (d)[d] | Q.M. ∇(ESPOT)[b] |
|---|---|---|---|
| | Electronegative Regions | | |
| $H_3N$ | 0.092 | 0.050 | 0.102 |
| $H_2O$ | 0.066 | 0.040 | 0.073 |
| HF | 0.038 | 0.030 | 0.039 |
| $H_3P$ | 0.063 | 0.019 | 0.037 |
| $H_2S$ | 0.038 | 0.015 | 0.032 |
| HCl | 0.019 | 0.009 | 0.017 |
| | Electropositive Regions | | |
| $H_2NH$ | −0.010 | −0.010 | −0.023 |
| HOH | −0.019 | −0.019 | −0.037 |
| FH | −0.029 | −0.029 | −0.053 |
| $H_2PH$ | −0.001 | −0.001 | −0.001 |
| HSH | −0.008 | −0.008 | −0.021 |
| ClH | −0.015 | −0.015 | −0.039 |

[a] Electrostatic potential gradient = ESPOT($R$) − ESPOT($R$ + 1), where $R$ is the appropriate reference position (see Table VII); representation (c) used. [b] Same as in footnote *a*, but gradient evaluated using the quantum mechanically derived wave functions of ref 1. [c] Evaluated using simple charge distribution (c); see Figure 1. [d] Evaluated using simple charge distribution (d); see Figure 1.

the molecules discussed here. As in Table IX, we have evaluated *finite* gradients, since this allows a more accurate estimate for the interaction energy of the relevant dipolar molecule. As noted before, the relative order of the gradients generally follows that of ESPOT, but one particular example is worth discussing in detail. The two N-H bonds in formamide have very different electrostatic potentials (0.050 vs. 0.010 au/Å) depending on whether they are trans or cis to the -C=O. However, their ∇(ESPOT) are comparable, consistent with the fact that both form comparable strength H bonds to $H_2O$.[28] The trans N-H would be expected to interact much more strongly with an *anion*.

**B. Choice of Reference Position.** In our earlier study of H bonding,[1] reference positions of 4 au (2.12 Å) for first row bases and 5 au (2.65 Å) for second row bases and 2 Å for A-H acids were used. More recently,[2] we have shown that one can use the van der Waals radius of the bases or the electrostatic potential minimum as "reference positions" and the relative order of electrostatic potentials is preserved for the hydrides. However, in certain cases ($\Delta E$($H_2CO$···HF) vs. $\Delta E$(HCN···HF)) we predict the incorrect order unless we take into account[2] the fact that for $H_2O$···HF $R$(O-F) = 2.73 Å and for H-CN···HF $R$(N-F) = 2.90 Å. Thus, the use of different reference points for different acids and bases is appropriate for cases where we have available theoretical or experimental data suggesting different minimum energy geometries.

**C. Equations for ∇(ESPOT).** Because it is straightforward to use the electrostatic potential gradients instead of the electrostatic potentials, we can immediately suggest their use in the equations

$$-\Delta E = 3070 \times \nabla(\text{POTA}) \times \nabla(\text{POTB}) \quad (6)$$

$$-\Delta E = 4230 \times \nabla(\text{POTA}) \times \nabla(\text{POTB}) \quad (7)$$

The constant in eq 6 is determined to have the quantum mechanically calculated gradients for $H_2O$ reproduce the calculated $\Delta E$ for dimerization of $H_2O$ with that basis set (8.1 kcal/mol); the constant in eq 7 is determined in order to reproduce the "experimental" $(H_2O)_2$ dimerization energy (5.3 kcal/mol) with simple charge choice (c) (Table X).

**D. A Detailed Comparison of These Approaches for $\Delta E$($H_2O$···HOH) vs. $\Delta E$(HCN···HCN).** To illustrate the pitfalls

**Table X.** Electrostatic Potential Gradients for the Molecules Considered in Table VII

| Molecule | ∇(ESPOT)[a] | θ, deg[b] |
|---|---|---|
| | Electronegative Regions | |
| $H_3N$ | 0.092 | 0 |
| $H_2O$ | 0.066 | 57 |
| HF | 0.038 | 60 |
| $H_3P$ | 0.063 | 0 |
| $H_2S$ | 0.038 | 60 |
| HCl | 0.019 | 70 |
| $F^-$ | 0.151 | |
| $F_2$ | 0.007 | 75 |
| $H_2$ | 0.005 | π |
| $N_2$ | 0.028 | 0 |
| HCN | 0.056 | 0 |
| HNC | 0.050 | 0 |
| $H_2CO$ | 0.052 | 60 |
| $H_2CO(n\rightarrow\pi^*)$ | 0.014 | π(C) |
| $H_2CO(\pi\rightarrow\pi^*)$ | 0.014 | 60 |
| $H_2NCHO$ | 0.065 | lp trans |
| $H_2NCHO$ | 0.066 | lp cis |
| $H_2NCHO$ | 0.023 | π − 0 |
| $CH_3NH_2$ | 0.089 | (0) |
| $CH_3OH$ | 0.064 | (57) |
| $CH_3F$ | 0.037 | (60) |
| $C_2H_4$ | 0.011 | π |
| $C_2H_2$ | 0.007 | π |
| $SO_2$ | 0.040 | lp |
| $CO_2$ | 0.031 | 60 |
| | Electropositive Regions | |
| F-H | −0.029 | (0) |
| HO-H | −0.019 | (0) |
| $H_2N$-H | −0.010 | (0) |
| Cl-H | −0.015 | (0) |
| HS-H | −0.008 | (0) |
| $H_2P$-H | −0.001 | (0) |
| $H_3C$-H | −0.002 | (0) |
| $F_3C$-H | −0.021 | (0) |
| NC-H | −0.021 | (0) |
| CN-H | −0.025 | (0) |
| CHOHNH | −0.016 (−0.013) | (0) |
| $O_2S$ | −0.023 | 75 |
| $O_2C$ | −0.009 | π(C) |
| $H_2$ | −0.002 | 0 |
| $F_2$ | −0.004 | 0 |
| $N_2$ | −0.006 | π |
| $H_3N^+$-H | −0.090 | (0) |
| $Li^+$ | −0.167 | |

[a] (ESPOT) is finite electrostatic potential gradient. This is determined by comparing the electrostatic potential at the reference position $R$ (Å) in Table VII and at the position ($R$ + 1) Å. ∇(ESPOT) = ESPOT($R$) − ESPOT($R$ + 1). Units are au/Å$^2$, representation (c) used. [b] The optimum angular orientation, where ∇(ESPOT) is most *positive* for electronegative regions and most *negative* for electropositive regions. In the case of the A-H Lewis acids, we only report the gradient along the A-H bond, but see Table VI for a description of the nonlinearity of ∇(ESPOT) for some of the hydrides. See also the corresponding footnotes in Table VII for explanations of θ.

of simple "predictions" for $\Delta E$'s, we compare the dimerization of HCN and $H_2O$ (Table XI). Unfortunately, the experimental dimerization energy at 0 K is not well established for either, but reasonable estimates suggest a $-\Delta E$ of ~5.3 kcal/mol for $(H_2O)_2$ and 4.3 kcal/mol for $(HCN)_2$.[29]

Application of either eq 3 or 7 using the same reference position overestimates the relative dimerization energy of HCN, but a simple correction (for a point dipole, the electrostatic potential changes as $1/R^2$ and the gradient as $1/R^3$ where $R$ is the distance from the molecule)[30] to either equation, taking into account that $R$(H···O) in the water dimer is 2.047 Å and $R$(H···N) in $(HCN)_2$ is near 2.343 Å,[31] correctly pre-

**Table XI.** A Comparison of the Calculation of Energy of Dimerization of $H_2O$ and HC≡N (kcal/mol)

| | $-\Delta E°$ $((H_2O)_2)$ | $-\Delta E°$ $((HCN)_2)$ |
|---|---|---|
| Equation 2[a] | (5.3) | (7.5) |
| Equation 6[b] | (5.3) | 5.4 |
| Equation 2, correct for distance[c] | 5.5 | 4.5 |
| Equation 6, correct for distance[d] | 5.6 | 2.5 |
| Direct electrostatic calculation[e] | 6.8 | 4.9 |
| Quantum mechanical calculation[f] | 8.1 (5.9) | 5.8 (4.7) |
| "Experiment" [g] | 5.3 | 4.3 |

[a] Application of eq 2. Table IX; those found using the simple charge. [b] Application of eq 6; ∇(ESPOT) for $H_2O$ are in representation of HCN (Figure 7) are −0.056 (electronegative region) and 0.023 (electropositive region). [c] Use eq 2, but correcting for differences in geometry as described in text. [d] Use eq 6, but correcting for differences in geometry as described in text. [e] $\Delta E((H_2O)_2)$ from Table III. $\Delta E((HCN)_2)$ evaluated using the charge distribution in Figure 7, the two molecules collinear and $R$(C···N) = 3.3 Å. [f] Values in parentheses, STO-3G ab initio calculations described in ref 33; values not in parentheses from ref 1 ($(H_2O)_2$) and unpublished results $(HCN)_2$); both of these were found using a 431G basis set. [g] Estimated as described in footnote 31.

dicts that $-\Delta E((H_2O)_2) > -\Delta E((HCN)_2)$. This same result is found when we use our simple charge distribution and calculate $-\Delta E(HCN)_2)$ as we have for the 36 dimers (fixing $R$(C···N) = 3.3 Å). Both the complete electrostatic calculations and the quantum mechanical calculations (Table XI) correctly find that the water dimer H bond is stronger than the HCN dimer H bond.

In summary, one can use eq 3 and 7 as first-order "guesses" to compare dimerization energies. Using the entries in Table VII (or corresponding gradients in Table X) one can predict the $-\Delta E$ for 414 (23 × 18) acid–base complexes. However, one can also use knowledge of experimental distances where available to refine such predictions. A final step is merely to evaluate the relative electrostatic interaction energy for the various dimers. If simple applications of eq 3 or 7 suggest that the $\Delta E$'s are very different, more refined applications are not really crucial.

We should, however, stress some of the limitations of this approach.[2] Equations 2–7 all suggest that, for example, if a given Lewis base interacts more strongly with one Lewis acid than another, it will interact more strongly with all Lewis acids than the second. Both Umeyama and Morokuma[13] and we[2,23] have documented exceptions to this in very strong complexes ($H^+$ and $Li^+$ affinities of Lewis bases), and those that involve substantial geometry reorganization of the fragments. Another important exception is the overestimate (with both the quantum mechanically and simply derived electrostatic potentials) of the Lewis acid strength of a C–H bond. This comes about because of our choice of a standard choice of 2 Å for the reference potential from the proton in all A–H, whereas for $F_3C$–H···$NH_3$ H···N is calculated to be 2.3 Å and for F–H···$NH_3$ $R$(H···N) is calculated to be 1.7 Å.[1] In addition, exchange repulsion plays a very important role in the relative Lewis acidity of H-bonded complexes,[14] and that is one reason why the electrostatic potential and its gradient are less accurate at ordering Lewis acid than Lewis base strengths.[1,2]

## Comparison with Other Simple Charge Representations

Shipman and Scheraga[32] have developed an electron pair representation of the charge distribution in a number of simple molecules including $NH_3$, $CH_3NH_2$, $H_2O$, $CH_3OH$, and *n*-butane. Their approach was empirical: determine the location of the electron pairs and the parameters of the exp-6 part of the potential to reproduce a number of experimental properties. The location of their electron pairs differs considerably from ours; for example, their bond pair in $H_2O$ is closer to H than O, but the corresponding lone pair is further from the oxygen than ours. Their approach also leads to reasonable H-bond dimerization energies and geometries.

Stillinger and Rahman[33] have proposed a simple empirical representation of the water charge distribution in order to carry out molecular dynamics calculations on $H_2O$ liquid. Their potential also leads to a reasonable H-bond dimerization energy and geometry for $H_2O$.

Tomasi and co-workers[34] have developed a set of transferable charges from ab initio calculations, which can reproduce the electrostatic potential calculated from the wave function. Their approach is more sophisticated than ours, but not as simply applicable.

An even simpler approach than ours is to use atom-centered partial charges and no explicit lone pairs. Most conformational analysis calculations use such sets of charges. We feel that one "needs" the lone pairs to correctly reproduce the structure of $(HF)_2$ and $(H_2O)_2$.[35]

We have used a valence bond approach (hybridized lone pairs) although implicitly using the ideas of MO theory (the $\sigma$–$\pi$ energy gap is important in the choice of lone pair angle for HF, HCl, $H_2O$, and $H_2S$). One can imagine other charge distributions where the $\pi$ electrons are represented explicitly and differently than the $\sigma$. In our approach, both $\sigma$ and $\pi$ electrons are already involved in bonding and thus do not have an explicit effect on intermolecular forces; lone pairs, on the other hand, are available for donation. However, our results for $C_2H_4$ and $C_2H_2$ suggest that further refinements of the $\pi$ electron representation are necessary if one desires as accurate a representation of these $\pi$ electrons as we have for $\sigma$ and n.

## Summary and Conclusions

We have presented an empirical approach to deriving a representation of the charge distribution in simple molecules and have shown that such an approach is capable of qualitatively reproducing trends in dimerization energy and geometry as well as relative electrostatic potentials for a number of such molecules. We have shown how such an approach can be applied to molecules containing $\sigma$ electrons, $\pi$ electrons, and n (nonbonded) electrons as well as molecules in excited states and those with a number of important resonance structures. Thus, we are in a position to make qualitative predictions (eq 3 and 7) of energy and geometry for a number of intermolecular complexes.

**Acknowledgments.** We gratefully acknowledge financial support from the NIH (GM-20564 and GM-70718) and the NSF (CHE 76-81718). We thank K. Janda and J. Tomasi for sending us manuscripts prior to publication and L. C. Allen for his comments on ref 2 which stimulated the initiation of this study.

## References and Notes

(1) P. Kollman, J. McKelvey, A. Johansson, and S. Rothenberg, *J. Am. Chem. Soc.*, **97**, 955 (1975).
(2) P. Kollman, *J. Am. Chem. Soc.*, **99**, 4875 (1977).
(3) R. Bonaccorsi, A. Pullman, E. Scrocco, and J. Tomasi, *Chem. Phys. Lett.*, **12**, 622 (1972).
(4) Recall that the electrostatic potential (ESPOT) at **R** due to a collection of $n$ test charges is $\sum_{i=1}^{n} q_i/|r_i - \mathbf{R}|$. Assuming no charge redistribution, a test charge $q_j$ placed at $R$ will have an interaction energy of $q_j \times$ ESPOT. The gradient of ESPOT = ∇(ESPOT) is a vector, but here we focus on its component in the particular directions relevant to intermolecular interactions; e.g., for A–H the gradient of the potential along the A–H bond direction will be of most interest to us. A test dipole, $\mu_T$, placed in an electrostatic potential gradient (∇(ESPOT)) will interact with an energy $\mu_T \cdot \nabla$(ESPOT).
(5) K. Morokuma, *J. Chem. Phys.*, **55**, 1236 (1971).
(6) H. Umeyama and K. Morokuma, *J. Am. Chem. Soc.*, **98**, 4400 (1976).
(7) See, for example, R. Drago, G. C. Vogel, and T. E. Needham, *J. Am. Chem. Soc.*, **93**, 6014 (1971).
(8) R. S. Mulliken and W. B. Person, "Molecular Complexes: A Lecture and Reprint Volume", Wiley-Interscience, New York, N.Y., 1969.
(9) L. C. Allen, *J. Am. Chem. Soc.*, **97**, 6921 (1975).

(10) See G. C. Pimentel and A. L. McClellan, "The Hydrogen Bond", W. H. Freeman, San Francisco, Calif., 1960, for a discussion of the "deficiencies" of an electrostatic model of the hydrogen bond.
(11) T. R. Dyke, B. J. Howard, and W. Klemperer, *J. Chem. Phys.*, **56**, 2442 (1972).
(12) D. R. Yarkony, S. V. O'Neill, and H. F. Schaefer, *J. Chem. Phys.*, **60**, 855 (1975).
(13) H. Umeyama and K. Morokuma, *J. Am. Chem. Soc.*, **99**, 1316 (1977).
(14) F. Cotton and G. Wilkinson, "Advanced Inorganic Chemistry", 3rd ed, Wiley-Interscience, New York, N.Y., 1972, describe the different electronegativity scales; we have used the Allred–Rockow scale.
(15) Of course, we could use any fraction of the van der Waals distance, so these choices are just representative values.
(16) We used experimental monomer geometries for these molecules; see ref 1.
(17) As discussed in ref 1 and 2, we evaluated the electrostatic potential around the periphery of the molecule and found suitable "reference positions" to compare the Lewis acidity and basicity of various molecules. For electrophilic regions, we found that an appropriate choice of distances from atoms were H, 2 Å; C, Cl, S, N, F = 2.65 Å. For nucleophilic regions: N, O, F = 2.12 Å and Cl, S, P = 2.65 Å. In each case, we choose the optimum *angular* orientation at this distance from the atom.
(18) K. Janda, J. M. Steed, S. E. Novick, and W. Klemperer, submitted for publication.
(19) According to the vdW model, it is a stronger Lewis base than HF; with the $\frac{1}{2}$ vdW model, it is weaker than HF.
(20) B. J. Rosenberg, W. C. Ermler, and I. Shavitt, *J. Chem. Phys.*, **65**, 4072 (1976).
(21) H. Kistenmacher, H. Popkie, and E. Clementi, *J. Chem. Phys.*, **58**, 5627 (1973).
(22) One might speculate at this point that the tendency for $H_2PH\cdots PH_3$ to have a linear H bond rather than be bifurcated in the 431G calculations is due to charge transfer terms (which would favor a linear A–H···B geometry) canceling the electrostatic tendency to bifurcate. As has been previously noted,[2] such charge redistribution effects would be expected to be more important in second row (P, Cl, S) than first row (N, O, F) intermolecular complexes.
(23) P. Kollman and S. Rothenberg, *J. Am. Chem. Soc.*, **99**, 1333 (1977).
(24) S. Iwata and K. Morokuma, *J. Am. Chem. Soc.*, **95**, 7563 (1973).
(25) K. G. Spears, *J. Phys. Chem.*, **81**, 186 (1977).
(26) J. Del Bene, *J. Chem. Phys.*, **62**, 4666 (1975).
(27) H. Bent, *Chem. Rev.*, **68**, 587 (1968).
(28) A. Johansson, P. Kollman, S. Rothenberg, and J. McKelvey, *J. Am. Chem. Soc.*, **96**, 3794 (1974).
(29) The estimate for $(H_2O)_2$ comes from an analysis by P. Kollman in "Modern Theoretical Chemistry", Vol. 7, H. F. Schaefer, Ed., Plenum Press, New York, N.Y., 1977. For $(HCN)_2$, W. F. Giaque and R. A. Ruhrwein (*J. Am. Chem. Soc.*, **61**, 2626 (1939)) found $\Delta H^{298} = -3.3$ kcal/mol; using an approximate (1 kcal/mol) difference between $\Delta H^{298}$ and $\Delta E^{\circ}$ as was found in the above analysis for $(H_2O)_2$), we conclude that $-\Delta E^{\circ}$ for $(HCN)_2$ is likely to be ~4.3 kcal/mol.
(30) Comparing the expected distance dependence with that actually calculated with these charge distributions indicates that the electrostatic potential at these distances from the molecule follows approximately the very simple $1/R^2$ dependence.
(31) STO-3G calculations on $(HCN)_2$ (A. Johansson, P. Kollman, and S. Rothenberg, *Theor. Chim. Acta*, **26**, 97 (1972)) and $(H_2O)_2$ (J. Del Bene and J. A. Pople, *J. Chem. Phys.*, **52**, 4858 (1970)) suggest that $R(N\cdots C) > R(O\cdots O)$ by ~0.4 Å. Thus, we have used the observed O–O distance in $(H_2O)_2$ ($R = 3.0$ Å) and assumed $R(C-N) = 3.4$ Å. This leads to an H···O distance in $(H_2O)_2$ of 2.047 Å and an H···N distance in $(HCN)_2$ of 2.343 Å. We then scale the Lewis acid ESPOT from Table VI by $(2.0\text{ Å}/R(H\cdots X))^n$, and the Lewis base ESPOT by $(2.12\text{ Å}/R(H\cdots X))^n$ where $n = 2$ for ESPOT and $n = 3$ for $\nabla$(ESPOT).
(32) L. Shipman and H. A. Scheraga, *Proc. Natl. Acad. Sci. U.S.A.*, **72**, 543 (1975).
(33) F. Stillinger and A. Rahman, *J. Chem. Phys.*, **60**, 1545 (1974).
(34) R. Bonaccorsi, E. Scrocco, and J. Tomasi, *J. Am. Chem. Soc.*, **98**, 4049 (1976); submitted.
(35) J. O. Noell and K. Morokuma (*J. Phys. Chem.*, **80**, 2675 (1976)) also found $\theta = 20$ for $(H_2O)_2$ with atom-centered partial charges and $R$(O–O) fixed. However, the experimental fact that $\theta > 20$ for $(H_2O)_2$ and $\theta \neq 0$ for $(HF)_2$ suggests that a nonsymmetric charge distribution around F and O is required.

# Symmetry Numbers, Not Statistical Factors, Should Be Used in Absolute Rate Theory and in Brønsted Relations

**Eli Pollak and Philip Pechukas***

*Contribution from the Department of Chemistry, Columbia University, New York, New York 10027.* *Received June 2, 1977*

**Abstract:** For many years there has been some question whether one should correct for the effects of molecular symmetry, in the rate expressions of transition state theory, by simply using symmetry numbers, as one does in the equilibrium expressions of statistical thermodynamics; several authors have asserted that the correct rate expressions should instead contain "statistical factors", which are dynamically defined numbers characteristic of the reaction mechanism. We show that the use of symmetry numbers is always correct, and that statistical factor rate expressions—when they differ from their symmetry number counterparts—are wrong. Special attention is given to reactions involving optically active species, and to symmetric reactions, where it is easy to make mistakes in writing down transition state theory rate expressions. The implications for the Brønsted relations of acid–base catalysis are discussed.

## I. Introduction

Over the past 15 years it has become widely accepted that in applications of absolute rate theory the symmetry of a reacting species or transition state is not always correctly taken into account by the use of symmetry numbers.[1-7] Two particular objections to the use of symmetry numbers have been raised: first, the symmetry number method seems to give clearly incorrect rate expressions for symmetric reactions;[1-3,6,8] and second, complications arise for reactions that involve optically active species.[1-3,6,9-12] Several authors have therefore proposed that one should use so-called "statistical factors" or "reaction path degeneracies" instead of symmetry numbers;[1-3,6] the definition of statistical factors seems to ensure that one obtains correct expressions in these cases.

More recently, however, a number of authors[6,13-15] have pointed out that the use of statistical factors cannot always be correct, for in some reactions the ratio of forward to backward rate constant—when these are evaluated using statistical factors—does not equal the equilibrium constant. There is therefore a puzzle: apparently symmetry numbers are not always enough but on the other hand statistical factors can also lead to error; what then is the correct way of accounting for symmetry in transition state theory?

In this paper we show that the symmetry number method, properly applied, will always lead to correct rate expressions. Statistical factor rate expressions, when they differ from their symmetry number counterparts, are therefore wrong.

We emphasize that the suspicious phrase "properly applied", in the paragraph above, is not meant to cover magic or fraud. The rate expressions given by the symmetry number method are unambiguous, and they are correct, but it is easy to make mistakes writing them down for symmetric reactions and for reactions involving optically active species.

0002-7863/78/1500-2984$01.00/0 